Numerical Modeling of Geogrid Reinforced Soil Bed under Strip Footings using Finite Element Analysis

Ahmed M. Gamal, Adel M. Belal, S. A. Elsoud,

Abstract—This article aims to study the effect of reinforcement inclusions (geogrids) on the sand dunes bearing capacity under strip footings. In this research experimental physical model was carried out to study the effect of the first geogrid reinforcement depth (u/B), the spacing between the reinforcement (h/B) and its extension relative to the footing length (L/B) on the mobilized bearing capacity. This paper presents the numerical modeling using the commercial finite element package (PLAXIS version 8.2) to simulate the laboratory physical model, studying the same parameters previously handled in the experimental work (u/B, L/B & h/B) for the purpose of validation.

In this study the soil, the geogrid, the interface element and the boundary condition are discussed with a set of finite element results and the validation. Then the validated FEM used for studying real material and dimensions of strip foundation.

Based on the Experimental and numerical investigation results, a significant increase in the bearing capacity of footings due to an appropriate location of the inclusions in sand. The optimum embedment depth of the first reinforcement layer (u/B) equal to 0.25. The optimum spacing between each successive reinforcement layer (h/B) equal to 0.75 B. The optimum Length of the reinforcement layer (L/B) equal to 7.5 B. The optimum number of reinforcement is equal to 4 layers.

The study showed a directly proportional relation between the number of reinforcement layer and the Bearing Capacity Ratio BCR, and an inversely proportional relation between the footing width and the BCR.

Keywords— Reinforced soil, geogrid, Sand Dunes, Bearing Capacity.

1. INTRODUCTION

Soil improvement techniques such soil reinforcing systems are used to increase the bearing capacity of the soil and to reduce the structures settlement. Geosynthetics have been increasingly used as reinforcing construction materials in civil engineering projects such as roads, retaining walls, landfills, etc. Now, many types of products (geogrid, geotextile, geocell, geomembrane, etc.) are available in the engineering process. Each product is designed to solve a particular range of civil engineering problems. The most important purpose of using Geosynthetic reinforcement is to support load either static or dynamic and increase the soil bearing capacity

Many researches have been carried out to understand the beneficial effects of using reinforcement in soil, such as A.M El-Shesheny (2015) [1], A. Zidan (2012) [2], G. Madhavi Latha, Amit Somwanshi (2009) [3], Radhey Sharma (2009) [4], Saeed Alamshahi (2009) [5], Sao-Jeng Chao (2009) [6], S. Marandi, M. Bagheripour (2008) [7], A. R. Al-Sinaidi and A. H. Ali (2006) [8], A. Asakereh, S. M. Tafreshi, and M. Ghazavi (2012) [9], Basudhar, P.K., Saha, S., Deb, K (2007) [10], El Sawwaf, M.A (2007) [11], Boushehrian, Michalowski R. L. (2004) [12] Boushehrian, J.H., Hataf, N (2003) [13], Yetimoglu, T.,Wu, J.T.H., Saglamer (1994) [14]

Many experimental, numerical, and analytical studies have been performed to investigate the behavior of reinforced soil foundation (RSF) for different soil types. However, the behavior of reinforced soil under the foundation has not been established yet.

Ahmed M. Gamal, Graduate student (eng.gamal88@gmail.com),
Adel M. Belal , Prof. and Chair, (adel.belal@aast.edu),
S. A. Elsoud, Assoc. Prof. (saelsoud@gmail.com).

Construction and Building Engineering Department,
College of Engineering and technology
Arab Academy for Science and Technology and Maritime Transport,
Cairo- Egypt

2. FINITE ELEMENT MODELLING

Full modeling of soil, reinforcing elements, footing and loading are performed using commercial FEM package PLAXIS Version 8.2.

2.1 Material modeling

2.1.1 Soil constitutive law

The well-known Mohr-coulomb model has been considered as a first order approximation of real soil behavior. This elasto-plastic model requires the parameters shown in Table 1.

Unit weight	17.78 kN/m^3
Young's modulus [E_{ref}]	25000 kN/m^2
Poisson ratio [v(nu)]	0.35
Cohesion [C_{ref}]	15 kN/m^2
Friction angle [ϕ]	30°
Dilatancy angle [Ψ]	0°

Table 1: Soil parameters

2.1.2 Geogrid modeling

Geogrids are elastic flexible elements with a normal stiffness and no bending stiffness. These objects are generally used to model soil reinforcements. The geogrid was modeled using elasto-plastic constitutive model with the parameters shown in Table 2.

EA	500 kN/m
Np	45 kN/m

Table 2: Geogrid parameters

Where: EA: Axial/Normal Stiffness
Np: Ultimate tensile strength of the geogrid

2.1.3 Strip footing modeling

Six strip footings (A), (B), (C), (D), (H) & (L) with different dimensions are used as shown in Table3.

Model Footings (m)	
A	0.075
B	0.1
C	0.12
Full Scale Footings (m)	
D	1
H	3
L	5

Table 3: Strip footings model and real full scale dimensions

The steel strip footings (A), (B) & (C) are modeled as a plate with steel parameters shown in Table 4.

Plate Properties			
ϒ Steel	78.4	kN/m^3	
Modulus of Elasticity E	2E+08	kN/m^2	
Thickness (cm)	1	1	1
Width (cm)	7.5	10	12.5
EA – Axial Stiffness (kN/m)	150000	200000	250000
EI – Bending Stiffness (kN.m2/m)	1.25	1.6667	2.0833
Own Weight (kN/m/m)	0.0588	0.0784	0.098

Table 4: Steel plate footing parameters used in the FEM

The concrete strip footings (D), (H), (L) are modeled as a RC element with an interface elements with parameters shown in Table 5.

Material Model	Linear Elastic
Unit weight	23.563 kN/m3
Young's modulus [Eref]	2.482E+07 kN/m2
Poisson ratio [v(nu)]	0.25

Table5: Concrete footing parameters used in the FEM

2.1.4 Interface elements

The roughness of the interaction modeled by choosing a suitable value for the strength reduction factor in the interface (Rinner). This Factor relates the interface strength to the soil strength (friction angle and cohesion). An interface element between the soil and the geogrid had the typical value of Rinner =0.85 is used. This factor relates the interface strength to the soil strength. The value of the Rinner was chosen based on previous experience with the interaction between soils and geogrids which develop bearing and friction stresses. [M.A Sayed 2012]. The interface element between the soil and the steel plate was chosen rigid (Rinner =1) and between the concrete footing and the soil was chosen with the typical value of Rinner =0.6.

2.1.5 Boundary conditions

The modeled boundary conditions are assumed such that the vertical boundaries are free vertically and constrained horizontally while the bottom horizontal boundary is fully fixed as shown in Figure 1.

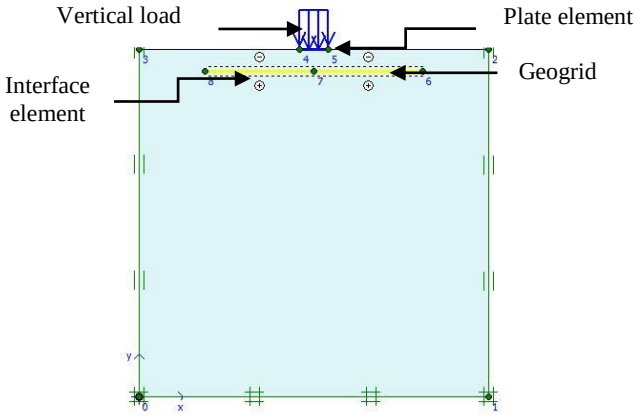

Fig 1: Finite element model showing the load and boundary conditions

2.1.6 Mesh Generation and initial conditions

Once the model geometry is defined and the material properties are assigned to all clusters and structural objects, the geometry inputs has to be divided into finite elements in order to perform finite element calculations. A refined mesh was adopted to minimize the effect of mesh dependency on the finite element modeling of cases involving changes in the number, length, and the location of geogrid layers. Figure 2 shows the mesh generation of the FEM.

The sand layer in this study was dry, so there was no need to enter ground water condition. The analysis does, however, require the generation of initial effective stresses by means of K0 = (1-sinϕ) procedure. Figure 3 shows the initial conditions for the FEM.

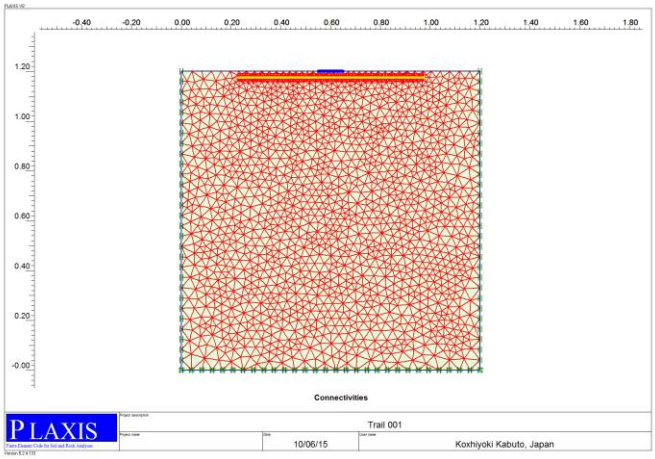

Figure 2: Mesh generation for the FEM.

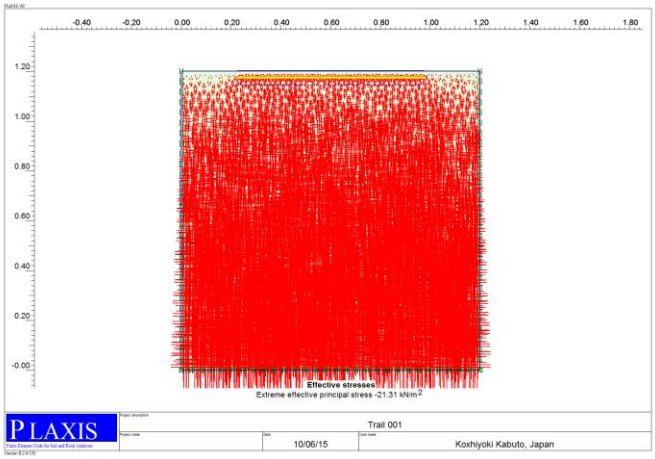

Figure 3: Total Stress generated in FEM

2.2 Finite Element Modeling Matrix

Figures 4 and 5 show the FEM matrix for the single and multi-reinforcement case which is the same matrix for the experimental study. In the Multi-layered case the FEM is created on footing (B) with h/B=0.75. Figure 6 shows the geogrid layout in the FEM, where (N) is the Number of reinforcement layers, (L) is the geogrid length, (u) the depth of the first layer measured from the bottom face of the footing, (h) the vertical spacing between consecutive layers of the reinforcement, and the footing width (B).

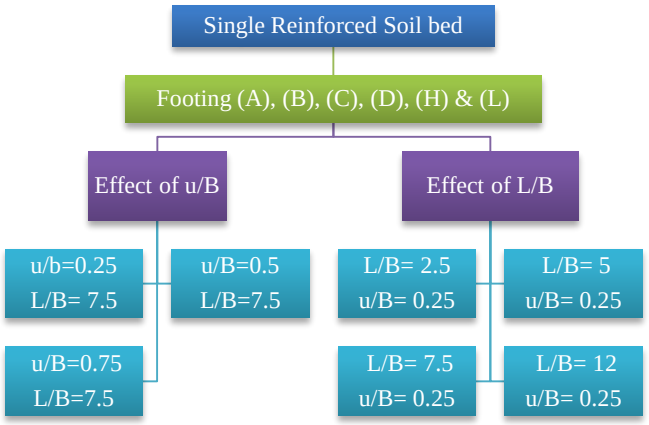

Figure 4: FEM Matrix (Single Layer Reinforced soil bed)

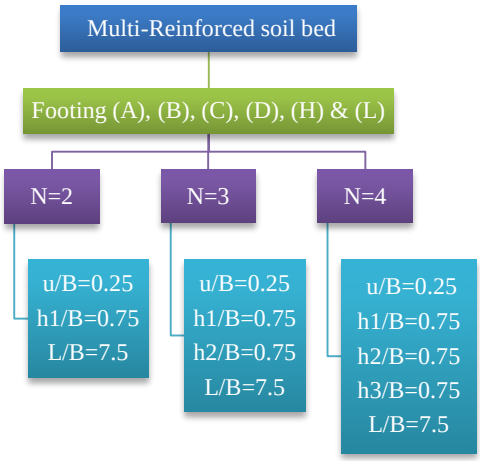

Figure 5: Experimental model Matrix (Multi-Reinforced soil bed)

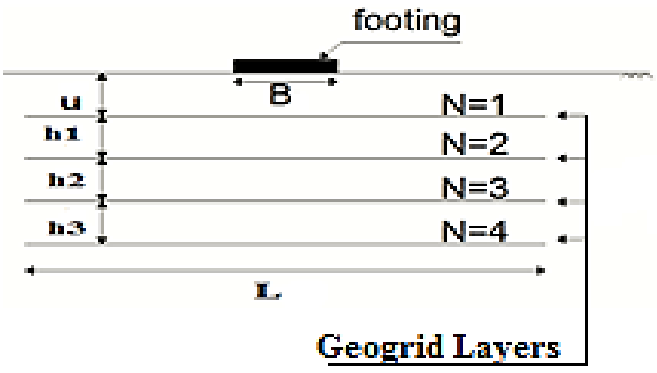

Figure 6: Geogrid Layout

2.3 FEM results Validation

The results are presented on the relation between the stresses under the footing in (KN/m^2) versus its associated settlement in (mm). Plaxis Calculations identifies the stress at failure with (X) sign and reports that the soil body collapsed.

Figures from 7 to 12 illustrate the comparison between the FEM and the experimental results for Unreinforced soil bed for footing (B) & N=1, L/B=7.5 and u/B=0.25 & N=1, u/B=0.25 and L/B= 5 & N=1, L/B=5 & u/B=0.25 & N=2, u/B=0.25, h1/B=0.75, & L/B=7.5 & N=3, u/B=0.25, h1/B= h2/B= 0.75, & L/B=7.5 & N=3, u/B=0.25, h1/B= h2/B= h3/B=0.75 & L/B=7.5

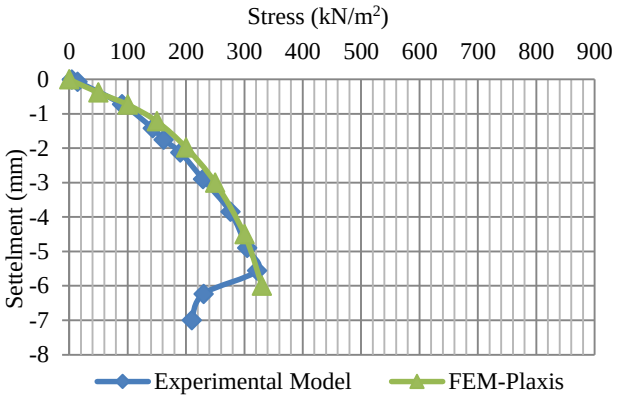

Figure 7: Unreinforced soil bed FEM vs. Experimental model results for footing (B)

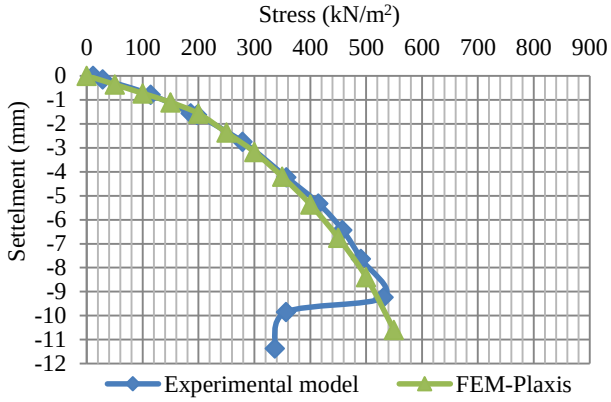

Figure 8: Footing (B) FEM vs. Experimental Model results with N=1, u/B=0.25 & L/B=7.5

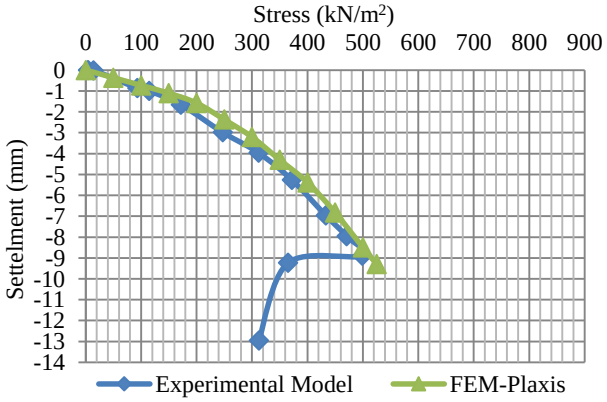

Figure 9: Footing (B) FEM vs. Experimental model results with N=1, L/B=5 & u/B=0.25

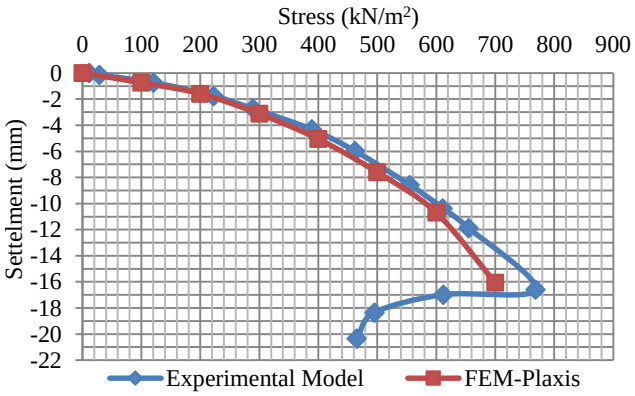

Figure 10: Footing (B) FEM vs. Experimental model results with N=2, u/B=0.25, h1/B=0.75, & L/B=7.5

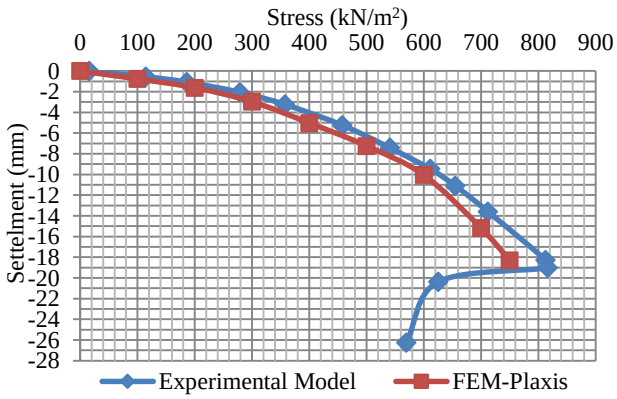

Figure 11: Footing (B) FEM vs. Experimental model results with N=3, u/B=0.25, h1/B= h2/B= 0.75, & L/B=7.5

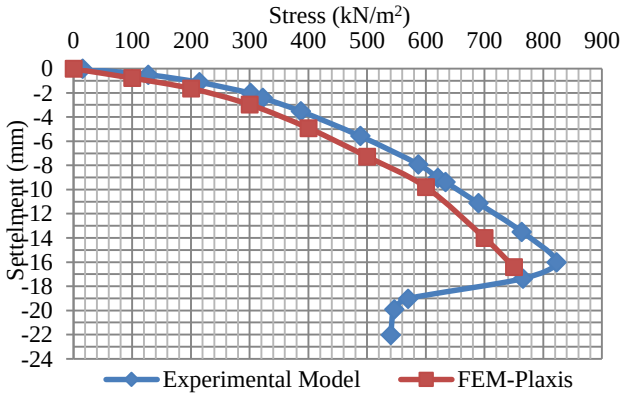

Figure 12: Footing (B) FEM vs. Experimental model results with N=3, u/B=0.25, h1/B= h2/B= h3/B=0.75 & L/B=7.5

It can be noticed from the comparison of the FEM and the experimental model results in the unreinforced, single reinforced and multi-reinforced soil bed that there is a medium agreement between the FEM and the experimental model results. Therefore the FEM is validated and ready for parametric study.

2.4 PLAXIS outputs

Other than stress (kN/m2) and Settlement (mm) curves, there are other outputs like the deformation mesh, Cartesian effective stresses, plastic points, horizontal and vertical displacements, Cartesian strains, Geogrid displacement and the tension in Geogrid. Figures 13 to 17 show the outputs for N=1, u/B=0.25 & L/B=7.5 with footing (B) at the ultimate stress value.

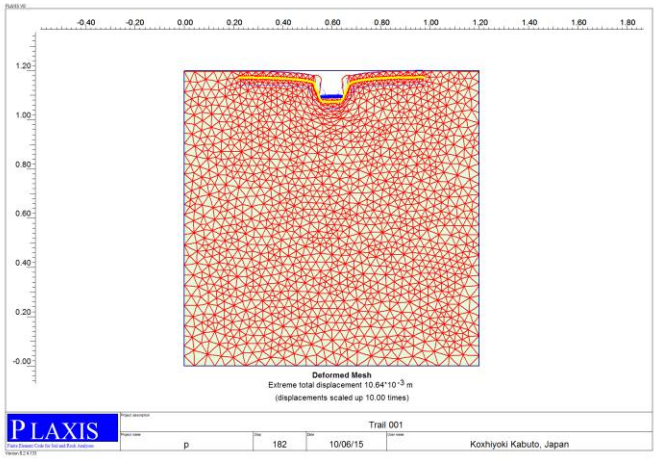

Figure 13: Deformed mesh

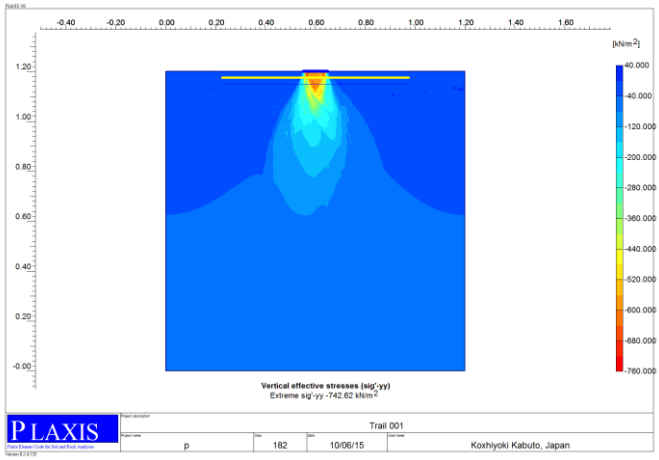

Figure 14: Effective Vertical Stresses (Sig'-yy)

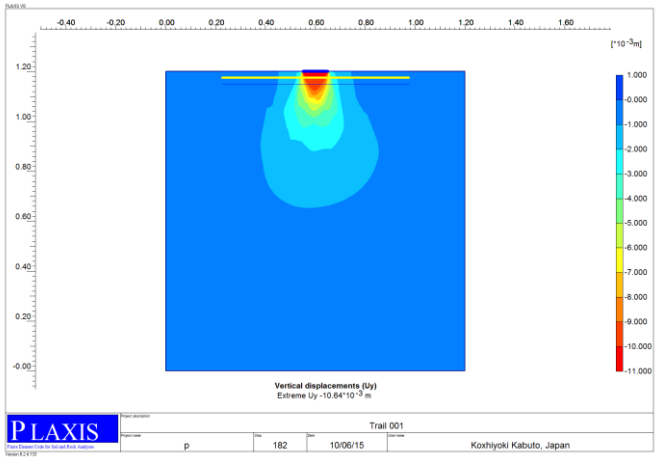

Figure 15: Vertical Displacements (Uy)

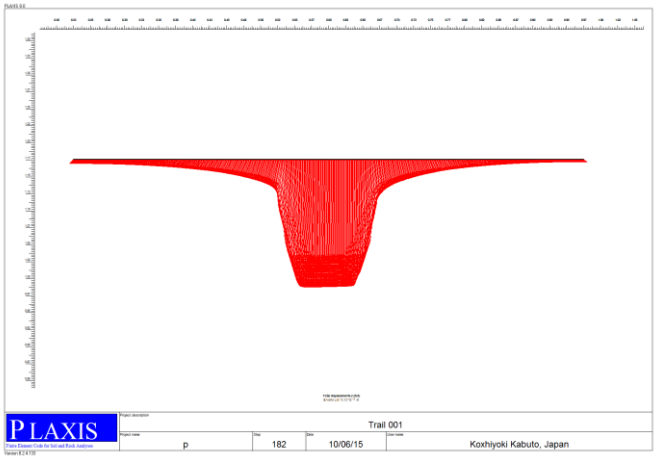

Figure 16: Geogrid displacement (Ulot)

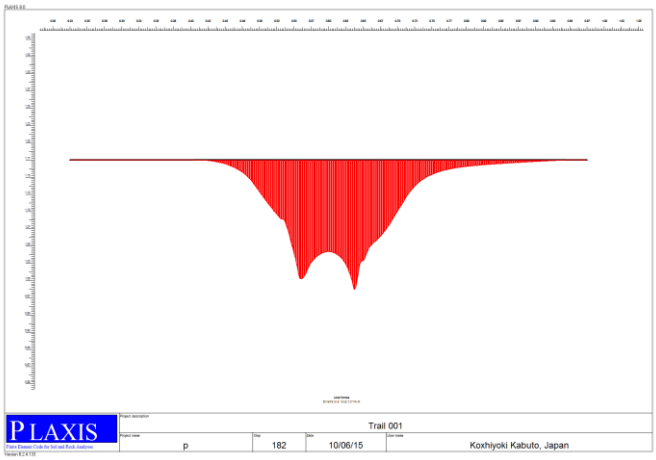

Figure 17: Geogrid axial forces

3. RESULTS, ANALYSIS AND DISSCUSION

Result analysis and comparison will be carried out and presented through the bearing capacity ratio (BCR). The improvement in the bearing capacity is represented using a non-dimensional factor, called bearing capacity ratio BCR. This factor is defined as the ratio of the footing ultimate pressure with reinforced bed (q reinforced) to the footing ultimate pressure with the unreinforced bed (q_{un} unreinforced).

3.1 Effect of first reinforcing layer depth (u/B):
The depth of the first reinforcing layer has been changed in terms of u/B=0.25, 0.5 & 0.75 for L/B=7.5 for footing (A), (B), (C), (D), (H) and (L) to get the optimum depth. Figure 18 illustrates the Bearing capacity ratio of the soil versus variable values of u/B for different footings. It is noticed that the values of (BCR) for u/B=0.25, and L/B=7.5 are 1.67, 1.67, 1.63, 1.18, 1.10 & 1.07 respectively, therefore 7%-70% improvement. That means as the width of the footing increase the improvement of the BCR decrease.

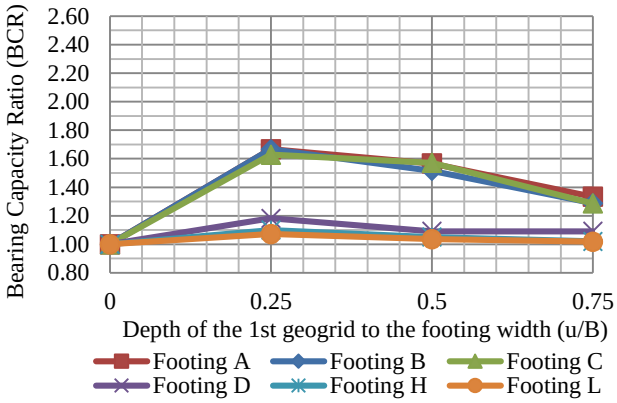

Figure 18: BCR vs. u/B for footing (A), (B), (C), (D), (H) & (L).

It can be concluded that the effect of using u/B = 0.25 is the optimum for footing (A), (B), (C), (D), (H) & (L).

3.2 Effect of reinforcing layers width (L/B):
The width of the first reinforcing layer has been changed in terms of L/B=2.5, 5, 7.5 & 12 for u/B=0.25 for footing (B), (D), (H) & (L) to get the optimum width. Figure 19 illustrates the BCR of the soil versus variable values of L/B for footings (B), (D), (H) & (L).

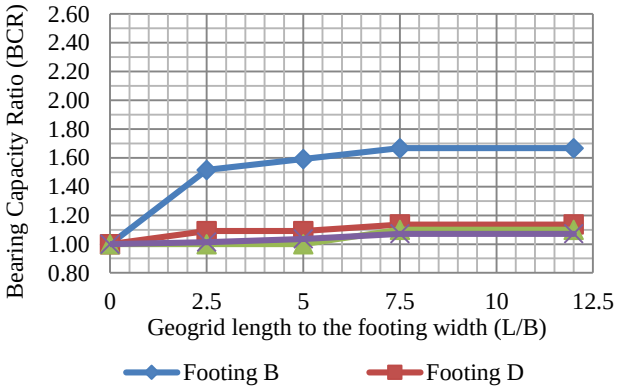

Figure 19: BCR vs. L/B for footing (B), (D), (H) & (L)

It is shown that from the finite element models, the effect of using L/B = 7.5 and 12 is almost the same therefore effect of using L/B=7.5 is the optimum for footing (B), (D), (H) & (L).

3.3 Effect of the spacing between the 1st & 2nd Geogrid (h1/B)
From Figure 20, it is noticed that the values of (BCR) for using two reinforcing layers with u/B=0.25, L/B=7.5 & h1/B=0.75 are 2.5, 2.12, 1.85, 1.32, 1.20 & 1.14. For footings (A), (B), (C), (D), (H) & (L) respectively, therefore 14%-150% improvement. That means as the width of the footing decrease the improvement of the BCR increase.

3.4 Effect of the spacing between the 2nd & 3rd Geogrid (h2/B)
From Figure 21 It is noticed that the values of (BCR) for using three reinforcing layers with u/B=0.25, L/B=7.5 & h1/B=0.75, h2/B=0.75 are 2.5, 2.27, 2.14, 1.36, 1.3 & 1.25 for footings (A), (B), (C), (D), (H) & (L) respectively, therefore 25%-150% improvement. That means as the width of the footing decrease the improvement of the BCR increase

3.5 Effect of the spacing between the 3rd & 4th Geogrid (h3/B)
From Figure 22 it is noticed that the values of (BCR) for using four reinforcing layers with u/B=0.25, L/B=7.5 & h1/B=0.75, h2/B=0.75 & h3/B=0.75 are 2.5, 2.27, 2.14, 1.36, 1.3 & 1.25 for footings (A), (B), (C), (D), (H) & (L) respectively, therefore 25%- 150% improvement. That means as the width of the footing decrease the improvement of the BCR increase.

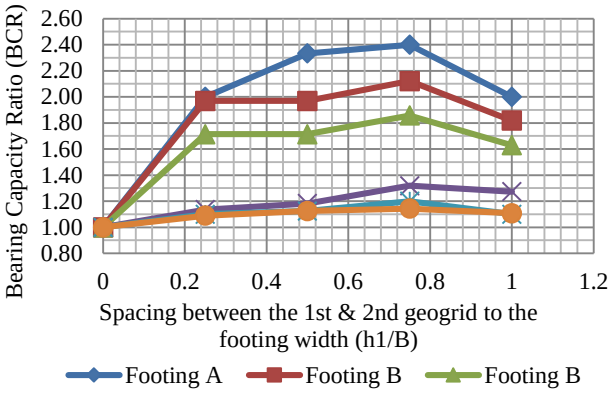

Figure 20: Bearing Capacity Ratio (BCR) vs. Spacing between the 1st & 2nd Geogrid to the footing width (h1/B) for footing (A), (B), (C), (D), (H) & (L)

It can be concluded from the experimental and finite element models that the effect of using h1/B = 0.75 is the optimum for footing (A), (B), (C), (D), (H) & (L)

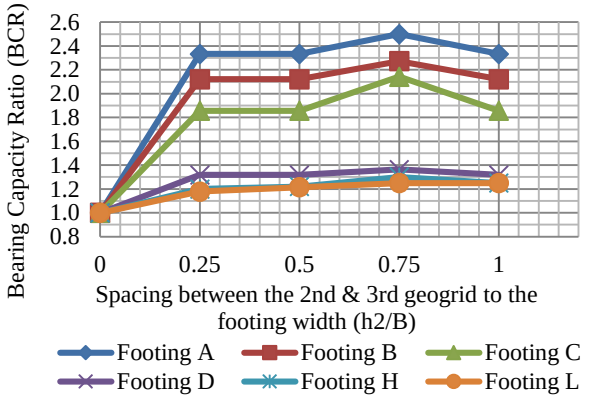

Figure 21: Bearing Capacity Ratio (BCR) vs. Spacing between the 2nd & 3rd Geogrid to the footing width (h2/B) for footing (A), (B), (C), (D), (H) & (L)

It can be concluded from the experimental and finite element models that the effect of using h2/B = 0.75 with h1=0.75 is the optimum for footing (A), (B), (C), (D), (H) & (L)

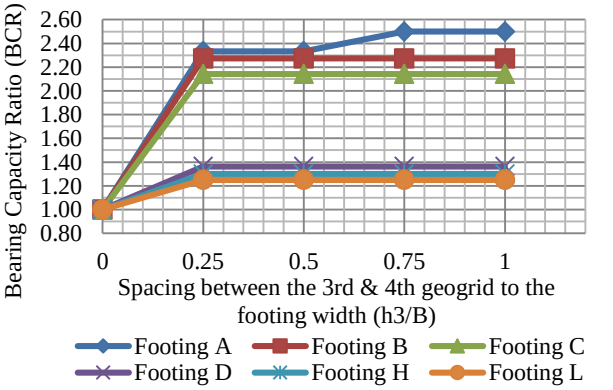

Figure 22: Bearing Capacity Ratio (BCR) vs. Spacing between the 3rd & 4th Geogrid to the footing width (h3/B) for footing (A), (B), (C), (D), (H) & (L)

It can be noticed that h3/B=0.25, 0.5, 0.75 & 1 having the same BCR for footing (A), (B), (C), (D), (H) & (L). Figure 23 and 24 illustrates the settlement (mm) for footings (A), (B), (C), (D), (H) & (L) in order to conclude the optimum value for h3/B

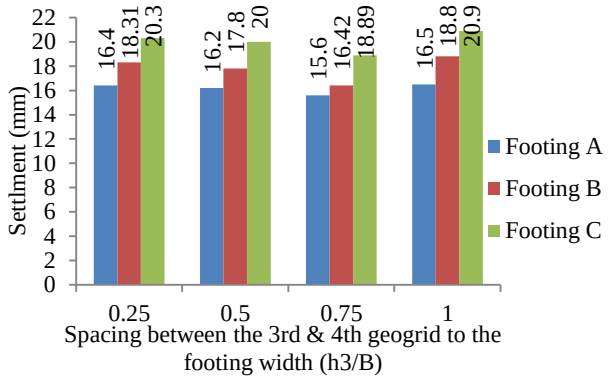

Figure 23: Settlement (mm) vs. Spacing between the 3rd & 4th Geogrid to the footing width (h3/B) for footing (A), (B) & (C)

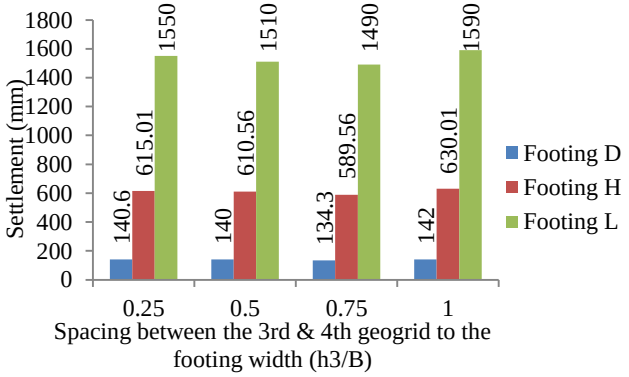

Figure 24: Settlement (mm) vs. Spacing between the 3rd & 4th Geogrid to the footing width (h3/B) for footing (D), (H) & (L).

It can be concluded that h3/B=0.75 is the least settlement, therefore it is the optimum.

3.6 Optimum No. of Reinforcement layers

Figure 25 & Figure 26 illustrates BCR and Settlement (mm) VS the no. of geogrids for footing (A), (B) & (C). It can be noticed that the BCR value increases with the increase of geogrids layer up to N=3. Figure 39 shows that the BCR value for N=3, 4, & 5 is the same for footing (A), (B) & (C), but the settlement (mm) for N=4 is less than the settlement for N=3, and for N=4 and 5 the is no significant change in settlement (mm) which can be concluded from Figure 27, therefore the optimum number of geogrids reinforcement is four for footing (A), (B) & (C).

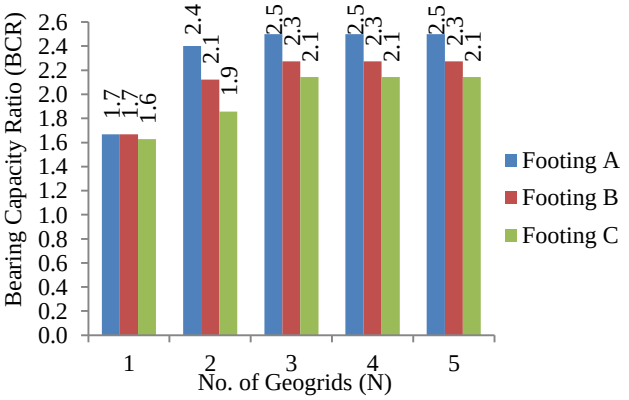

Figure 25: No. of Georgics (N) VS Bearing Capacity Ratio (BCR) for footing (A), (B) & (C)

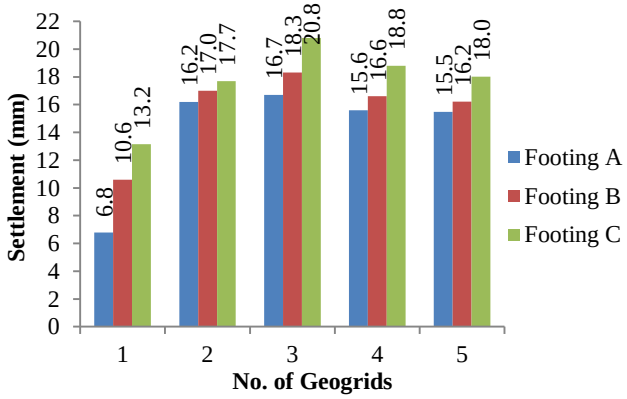

Figure 26: No. of Georgics VS Settlement (mm) for footing (A), (B) & (C)

Figure 27 & Figure 28 illustrates BCR and Settlement (mm) VS the no. of geogrids for footing (D), (H) & (L). It can be noticed that the BCR value increases with the increase of geogrids layer up to N=3, but the settlement (mm) for N=4 is less than the settlement for N=3, and for N=4 and 5 the is no significant change in settlement (mm) which can be concluded from Figure 29, therefore the optimum number of Geogrid reinforcement is four for footing (D), (H) & (L)

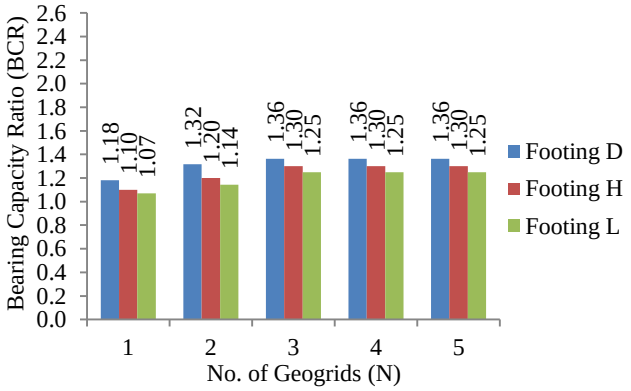

Figure 27: No. of Georgics (N) VS Bearing Capacity Ratio (BCR) for footing (D), (H) & (L)

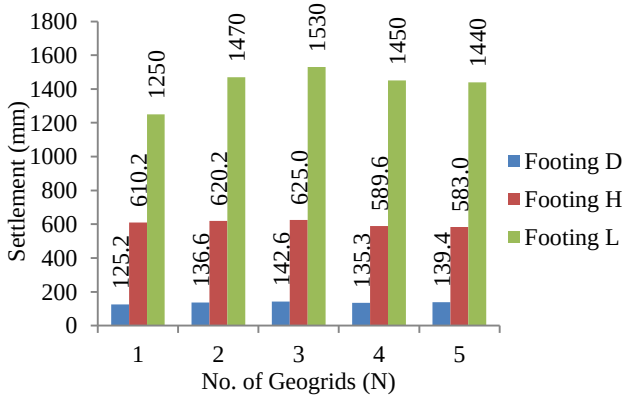

Figure 28: No. of Georgics VS Settlement (mm) for footing (D), (H) & (L)

From footing (A), (B), (C), (D), (H) & (L) it can be concluded that the optimum number of Geogrid layers to be used is four

4. CONCLUSIONS

Based on the Experimental and numerical investigation results, the following conclusions may be drawn.

1. The results of numerical modeling have shown that the provision of a reinforcement layer at an appropriate location in the body of sand dunes has resulted in a significant increase in the bearing capacity of footings.
2. The optimum embedment depth (u/B) of the first reinforcement layer which resulted in the maximum ultimate bearing capacity of the geogrid-reinforced soil bed was about 0.25 times the width of the footing
3. The optimum spacing (h/B) between each successive reinforcement layer which resulted in the maximum ultimate bearing capacity of the geogrid-reinforced soil bed was about 0.75 times the width of the footing.
4. The optimum Length (L/B) of the reinforcement layer which resulted in the maximum ultimate bearing capacity of the geogrid-reinforced soil bed was about 7.5 times the width of the footing.
5. The results of model tests and numerical analyses have shown that the optimum number of reinforcement is 4 layers
6. A medium agreement between the experimental and numerical results on general trend of behavior and the critical values of the geogrid parameters is observed. The study showed a directly proportional relation between the number of reinforcement layer and the BCR, and an inversely proportional relation between the footing width and the BCR.

REFERENCES

[1]. A.M El-Shesheny “Finite Element Analysis of Reinforced Soil under Dynamic loads”, Feb 2015.

[2]. A. Zidan, "Numerical study of behavior of circular footing on geogrid-reinforced sand under static and dynamic Loading," Geotechnical and Geological Engineering, vol. 30, pp. 499-510, 2012.

[3]. G. Madhavi Latha, Amit Somwanshi “Effect of reinforcement form on the bearing capacity of square footings on sand”, Geotextiles and Geomembranes vol. 27, pp. 409–422, 2009

[4]. Radhey Sharma, Qiming Chen, Murad Abu-Farsak, Sungmin Yoon “Analytical modeling of geogrid reinforced soil foundation”, Geotextiles and Geomembranes vol. 27, pp. 63–72, 2009

[5]. Saeed Alamshahi, Nader Hataf “Bearing capacity of strip footings on sand slopes reinforced with geogrid and grid-anchor”, Geotextiles and Geomembranes vol. 27, pp. 217–226, 2009

[6]. Sao-Jeng Chao “Improving Bearing Capacity of Shallow Foundations on Weak Soils Utilizing Geosynthetic Reinforcing Technique”, GeoHunan International Conference (2009) 40-46

[7]. S. Marandi, M. Bagheripour, R. Rahgozar, and A. Ghirian, "Numerical Investigation Into The Behavior of Circular Pad Shallow Foundations Supported By Geogrid Reinforced Sand," American Journal of Applied Sciences, vol. 5, p. 355, 2008.

[8]. A. R. Al-Sinaidi and A. H. Ali, "Improvement in bearing capacity of soil by geogrid-an experimental approach," IAEG2006, United Kingdom, 2006.

[9]. A. Asakereh, S. M. Tafreshi, and M. Ghazavi, "Strip footing behavior on reinforced sand with void subjected to repeated loading," International Journal of Civil Engineering, vol. 10, pp. 139-152, 2012

[10]. Basudhar, P.K., Saha, S., Deb, K., "Circular footings resting on geotextile-reinforced sand bed". Geotextiles and Geomembranes vol 25 (6), pp.377–384, 2007
[11]. El Sawwaf, M.A., "Behavior of strip footing on geogrid-reinforced sand over a soft clay slope". Geotextiles and Geomembranes, vol 25 (1) , pp. 50–60, 2007
[12]. Michalowski R. L. "Limit loads on reinforced foundation soils." Journal of Geotechnical and Geoenvironmental Engineering, ASCE (2004) 381-390.
[13]. Boushehrian, J.H., Hataf, N., "Experimental and numerical investigation of the bearing capacity of model circular and ring footings on reinforced sand". Geotextiles and Geomembranes, vol 23 (2), pp.144–173, 2003
[14]. Yetimoglu, T., Wu, J.T.H., Saglamer, A., Bearing capacity of rectangular footings on geogrid-reinforced sand. Journal of Geotechnical Engineering, ASCE 120, 1994, 2083–2099.